Experimentally Restrained Wave Function Method within the Hartree-Fock Formalism

Sebastián-de-la-Peña, *Universidad Autónoma de Madrid*

Supervisors: Stasis Chuchurka, Andrei Benediktovitch, and Nina Rohringer, *FS-TUXS, DESY*

September 6, 2022

Abstract

Wavefunctions are at the core of the Schrodinger picture of quantum mechanics, since they provide enough information to fully describe a given quantum mechanical system. Quantum Chemistry is the branch of physics that applies quantum mechanics to molecular systems. Most of the techniques that are used in this field involve approximations, as the complexity of the system increases rapidly as we add more atoms and molecules. As a consequence, many numerical techniques have been developed to approach this problems, such as Hartree-Fock or DFT. Nevertheless, applying these techniques to excited states carries many obstacles, and computational limitations start to become an issue. In this project, we suggest a new alternative framework based on experimentally restrained solutions to the Hartree-Fock method that overcome some of the difficulties of molecular systems, solving most of the issues of Hartree-Fock based algorithms and allowing the fitting of empirical parameters. Additionally, we show how to use experimental dipole moments from X-ray emission phenomena to fit our simple theoretical model is possible for the manageable case of the water molecule.

Contents

1. Introduction

In quantum mechanics, the wavefunction plays an esential role in describing a system. In the case of electrons in molecules, this is even more intuitive, as these electronic waves can also be used to predict bond behaviour, chemical properties, or even interaction with light. Nevertheless, many-body problems in non-relativistic quantum mechanics are already a matter that only approximations can deal with, and these approximation usually involve relying on numerical simulations. Quantum chemistry [3] is the field within physics that uses quantum mechanics and many-body problem theory to explain and predict chemical properties of compouds. Nonetheless, the difficulty to describe excited states, and the rapid increase of the complexity of molecular systems limits the predictive power of the theories used so far, such as Density Function Theory (DFT) [11] or Hartree-Fock (HF) [3, 10]. It is for this reason that great interest has been recently risen among scientist to discover simpler alternatives to describe such systems, and we suggest using experimental guidance to succeed in that goal, that is, make use of experimental parameters to include corrections in our theory.

X-ray emission spectroscopy (XES) has proved to be a technique complementary to X-ray absorption spectroscopy (XAS) that provides valuable information about the electronic structure of the system [8, 9]. XES is a secondary process of photo-absorption, where an electron from the outer shell fills the hole left by an ionized photo-electron produced in a X-ray absorption process (see Fig. 1). From this emission process, a cross-section can be measured, and from it a dipole moment between these two states is inferred [6, 7]. Our goal is to use these experimentally inferred dipole moment observables to correct our HF-based model of the excited states of the water molecule. [1]

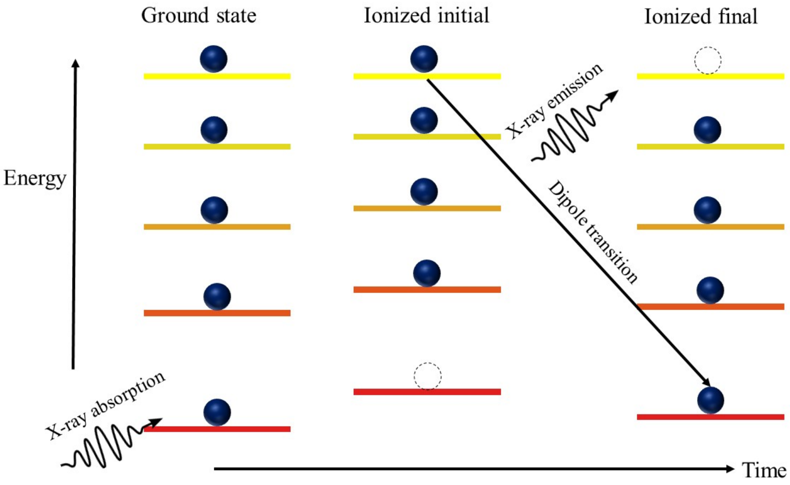

Figure 1: Schematic depiction of the processes involved in our model. First, an external X-ray photon absorption is produced by a core electron from the ground state. The core orbital becomes then a hole, that will be filled by an external shell electron. This outer-shell electron emits an X-ray photon that can be detected. In our example's model, this second electronic transition depends on the value of the dipole moment of the two states $|\boldsymbol{d}^{nm}|^2$.

Throughout this document, we present an original alternative based on recent methods of that involve fitting structure factors from X-ray diffraction [9], but in a general framework that allows different experimental parameters to be fitted simultaneously. Specifically, we will focus on dipole moments obtained from XES experiments that let us correct different excited states of a molecule. We provide in

---

[1] Initially, we aimed our project to explain XAS from inner shells to continuum, since that would allow us to describe the corrections to the ground state of the molecule as well. Yet, we found some difficulties regarding the computation of the dipole transitions (See App. B for more details). Fortunately, we can compute transitions between states where the number of electrons in the molecule is conserved and there is no ionization, and this was the motivation to study X-ray emission transitions between the electron-hole levels of molecules.

this document a quick review of the model used to prove our initial insight and a few examples where the code has been used. Sec. 2 will introduce the reader to the HF approximation and the restrain minimization formalism, whose detailed formulation can also be found in App. A. Sec. 3 will briefly explain the structure of the code and some results, and finally in Sec. 4 a summary of the document can be found.

2. Theoretical Introduction

2.1. The Hartree-Fock Approximation

For a given system of atoms, we can consider the nuclei as static particles, since their time scale is orders of magnitude larger than that of the electrons. This is known as the Born-Oppenheimer approximation. For a given nuclear distribution, we can now consider a system of electrons, which is a many-body quantum problem. For the sake of clarity, orbitals which implicitly include information about the spin-state of the electrons that occupy them will be referred to as *spin orbitals* , whereas those which contain merely information about the spatial distribution of the orbital will be called *spatial orbitals.* When we refer to orbitals that describe the electronic structure of a molecule, we call them *molecular orbitals*, while those obtained to describe single atoms are known as *atomic orbitals.* The Hartree-Fock approximation consists on using the intuitive notion of electrons filling energy levels (molecular orbitals), and leaving holes unfilled. Rigorously, this is expressed by assuming one single Slater determinant to describe the many-electron system, i.e., the total wavefunction of the molecule can be represented as $|\Psi_n\rangle = \frac{1}{\sqrt{N_n!}} \det \left(|\chi_1^{(n)}\rangle |\chi_2^{(n)}\rangle |\chi_3^{(n)}\rangle ... \right)$, where $\{|\chi_i\rangle\}$ are a set of spin molecular orbitals, and N_n is the total number of electrons. The remaining question of this model is which set of states $\{|\chi_i\rangle\}$ shall be used as molecular orbitals. To answer this question, the variational principle is used: *The set of molecular orbitals are such that the total energy of the system is stationary:*

$$\frac{\delta \langle \Psi_n | \hat{H} | \Psi_n \rangle}{\delta |\chi_i\rangle} = 0. \tag{1}$$

Eq. (1) will give us the HF equations. To express these equations in a numerically solvable form, we will use a specific basis as will be explained in the following sections.

In our system, the set of states we will work with have the same number of electrons N. These electrons will be distributed between spin-up and spin-down orbitals, so that we end up with N_α spin-up electrons and N_β spin-down electrons. In order to allow the computational calculation of the wavefunction, a finite basis needs to be chosen. This basis is typically made out of atomic orbitals, such as those of the atoms that compose the molecule, and the number of elements of the basis is K. As we increase the number of elements in our basis set we can get a better precision in our calculation.

2.2. HF-SCF Algorithm

For a given set of K atomic orbital basis, $\{|\phi_\mu\rangle\}$, we define the coefficent matrix for spin orbitals:

$$|\chi_p\rangle = C_{\mu p} |\phi_\mu\rangle \,, \tag{2}$$

and analogously for spatial orbitals:

$$|\psi_p^\alpha\rangle = C_{\mu p}^\alpha |\phi_\mu\rangle \,, \quad |\psi_p^\beta\rangle = C_{\mu p}^\beta |\phi_\mu\rangle \,. \tag{3}$$

Note that the same basis set is used for both spin-up and spin-down electrons. Here, $C_{\mu p}^\alpha$ and $C_{\mu p}^\beta$ are the coefficient matrices for spin-up and spin-down electrons, respectively; and $C_{\mu p}$ is the coefficient matrix written in spin orbital indexation. We can define the overlap matrix of the basis set as $S_{\mu\nu} = \langle \phi_\mu | \phi_\nu \rangle$.

Once the basis set has been chosen, the objetive of the HF method is to find $C^{\alpha,\beta}_{\mu p}$ such that the energy is minimized as in Eq. (1). The density matrix can be expressed using these coefficients as $D^{\alpha,\beta}_{\mu\nu} = C^{\alpha,\beta}_{\mu a} C^{\alpha,\beta\dagger}_{a\nu}$, where the sumation over a is done over the occupied orbitals. The HF method can be understood, instead of as an approximate solution (one single Slater determinant) to an exact Hamiltonian ($\hat{H}$), but as an exact solution to an approximate Hamiltonian. This new Hamiltonian is known as the *Fock operator* $\hat{F}$, and its expression in the spatial atomic orbitals is [3]:

$$F^{\alpha}_{\mu\nu} = h_{\mu\nu} + w_{\mu\mu'\nu\nu'}\left(D^{\alpha}_{\nu'\mu'} + D^{\beta}_{\nu'\mu'}\right) - w_{\mu\mu'\nu'\nu} D^{\alpha}_{\nu'\mu'},$$

$$F^{\beta}_{\mu\nu} = h_{\mu\nu} + w_{\mu\mu'\nu\nu'}\left(D^{\alpha}_{\nu'\mu'} + D^{\beta}_{\nu'\mu'}\right) - w_{\mu\mu'\nu'\nu} D^{\beta}_{\nu'\mu'} \quad (4)$$

The HF approximation allows us to transform the otherwise analitically unsolvable Schrodinger equation for a multielectronic system, into a Self-Consistent Field (SCF) algorithm, that is, an iterative method in which we pursue convergence of the variables. It is in this framework that we arrive at the Roothaan's equations for spin orbitals:

$$\boldsymbol{F}(\boldsymbol{C}_{\text{old}})\boldsymbol{C}_{\text{new}} = \boldsymbol{S}\boldsymbol{C}_{\text{new}}\boldsymbol{\epsilon}, \quad (5)$$

or the Pople–Nesbet–Berthier's equations for spatial orbitals:

$$\boldsymbol{F}(\boldsymbol{C}^{\alpha,\beta}_{\text{old}})\boldsymbol{C}^{\alpha}_{\text{new}} = \boldsymbol{S}\boldsymbol{C}^{\alpha}_{\text{new}}\boldsymbol{\epsilon}^{\alpha}_{\text{new}},\ \boldsymbol{F}(\boldsymbol{C}^{\alpha,\beta}_{\text{old}})\boldsymbol{C}^{\beta}_{\text{new}} = \boldsymbol{S}\boldsymbol{C}^{\beta}_{\text{new}}\boldsymbol{\epsilon}^{\beta}_{\text{new}}. \quad (6)$$

By solving these equations, one not only finds $C^{\alpha,\beta}_{\mu p}$, but also the energetic levels of the orbitals $\epsilon^{\alpha,\beta}_{p}$[2].

Once we have the new set of molecular orbitals from the previous equations, the occupied and virtual orbitals have to be determined. For each, α and β electrons, we have a set of K molecular orbitals materialized in their coefficients $C^{\alpha,\beta}_{\mu p}$ and their energies $\epsilon^{\alpha,\beta}_{p}$. Depending on whether the iterative method is done for the ground state or for excited states, we will have two different criteria to determine the occupied $N_{\alpha,\beta}$ molecular orbitals.

- *Aufbau principle:* For the ground state, we want to minimize the total energy of the system, and thus the occupied molecular orbitals which be chosen in such a way that the energy is the lowest. Therefore, orbitals with lower energy will be filled first.

- *Maximum Overlap Method:* In the case of excited states, the aufbau principle is of no use due to variational collapse to the ground state. We need thus a new criterion to choose the occupied and virtual orbitals from a given energetic spectrum in such a way that the global minimum is never reached, but local stationary states. The alternative we suggest is called *Maximum Overlap Method* (MOM) [2], and guarantees that our system will not sink in the ground state by picking those orbitals that overlap most with the span of the old occupied orbitals. The overlap formula for each molecular orbital is:

$$p_j = C^{\text{old}\dagger}_{a\mu} S_{\mu\nu} C^{\text{new}}_{\nu j}, \quad (7)$$

where the sum is also performed over a, and we will occupy the $N_{\alpha,\beta}$ with the molecular orbitals the maximize p_j.

---

[2] The Rothaan's equations are usually used in the Restricted HF scheme, while PNB equations are used for Unrestricted HF. Since we are interested in electornic configurations with an arbitrary number of electron in each spin state, we will make use of the UHF scheme.

The error can be determined via the error matrix defined as the commutator of the density matrix with the Fock operator:

$$\boldsymbol{e} = \boldsymbol{FDS} - \boldsymbol{SDF}, \tag{8}$$

and then taking the Frobenius norm of the error matrix $D_{rms} = ||\boldsymbol{e}||_{\mathrm{F}}$. Another alternative to evaluate the error D_{rms} is to check the convergence of the density matrix $D_{rms} = ||\boldsymbol{D}^{\mathrm{old}} - \boldsymbol{D}^{\mathrm{new}}||_{\mathrm{F}}$. The former criterion will be used only for DIIS purposes (as we will explain later), while the latter will be our generic criterion through most of the code.

2.2.1. Spin contamination

Due to the spin uncoupling of Eq. (6), after a finite number of iterations the system might end up not being an eigenstate of the total spin operator $\hat{S}^2$. This is because, in spite of the z spin component being defined by the difference between spin-up and spin-down electrons, the system has no constrain regarding the total spin, and this becomes a serious issue when we work with excited states. Nevertheless, any physical state must have a well defined total spin $\hat{S}^2$ due to $\left[\hat{H}, \hat{S}^2\right] = 0$. This effect that appears in the Unrestricted HF formalism is known as *spin contamination* [1]. The total spin of the electronic system when this effect is taken into account is given by:

$$\langle \hat{S}^2 \rangle = S_z^2 + S_z + N_\beta - \mathrm{Tr}\left(SD^\beta SD^\alpha\right). \tag{9}$$

The quantity to be minimized is $\mathrm{Tr}\left(SD^\beta SD^\alpha\right)$, which represents the overlap between the molecular orbitals of different spins. Once the minimization is performed including the minimized term as a correction to the Hamiltonian [1], a new term appears in Eq. (6) such that the modified Fock operator (that which includes the spin contamination corrections) becomes:

$$\tilde{F}^\alpha_{\mu\nu} = F^\alpha_{\mu\nu} - 2\lambda_\alpha S_{\mu\sigma} D^\beta_{\sigma\delta} S_{\delta\nu},\ \tilde{F}^\beta_{\mu\nu} = F^\beta_{\mu\nu} - 2\lambda_\beta S_{\mu\sigma} D^\alpha_{\sigma\delta} S_{\delta\nu}, \tag{10}$$

where λ_α and λ_β are the Lagrange multipliers of the restrained minimization.

2.2.2. DIIS method for improved SCF Convergence

In order to improve convergence, we also suggest using a method to accelerate SCF methods [4]. This method consists on using linear combinations density matrices of previous iterations (instead of simply the previous one), $\boldsymbol{D}_{\mathrm{new}} = c_i \boldsymbol{D}_i$, and determining the coefficients c_i by solving the following system of linear equations:

$$\begin{pmatrix} 0 & -1 & -1 & \dots & -1 \\ -1 & B_{11} & B_{12} & \dots & 0 \\ \dots & & & & \\ -1 & \dots & B_{ij} & & \\ \vdots & & & & \end{pmatrix} \begin{pmatrix} -\lambda \\ c_1 \\ \vdots \\ c_i \\ \vdots \end{pmatrix} = \begin{pmatrix} -1 \\ 0 \\ \vdots \\ 0 \\ \vdots \end{pmatrix}, \tag{11}$$

where $B_{ij} = \langle \boldsymbol{e}_i | \boldsymbol{e}_j \rangle$, λ is a Lagrange multiplier, and $\boldsymbol{e}_i$ are the error matrices of each iteration's density matrix:

$$\boldsymbol{e}_i = \boldsymbol{F}\boldsymbol{D}_i\boldsymbol{S} - \boldsymbol{S}\boldsymbol{D}_i\boldsymbol{F}. \tag{12}$$

This alogithm allows the error to decrase more rapidly than if we simply picked the last iteration's density matrix.

2.3. Coupled restrained minimization

In this report we are interested in X-ray emission spectroscopy process (XES), that is, emission of a photon from an outer-shell electron to an inner-shell hole, due to previous absorption in the system. This process' probability amplitude is related to dipole moment of the two excited states involved (Fig. 1). From the experimental cross-section, we can obtain the experimental value of the dipole moment between two different excited states m and n, $\boldsymbol{d}^{nm}_{\text{exp.}}$. The aim of this project is to numerically compute the wavefunction of these two excited states involved in the emission process by adding experimental restrains to the HF algorithm. To do so, we introduced a new potential that couples different excited states in such a way that the calculated dipole moment, $\boldsymbol{d}^{nm}_{\text{calc.}} = \langle\Psi_n|\hat{\boldsymbol{d}}|\Psi_m\rangle$ is pushed to fit the experimentally measured one:

$$L_n[|\Psi_n\rangle] = \langle\Psi_n|\,\hat{H} - E_n\,|\Psi_n\rangle + Q^{\text{d}}_n[|\Psi_n\rangle], \tag{13}$$

with $Q^{\text{d}}_n[|\Psi_n\rangle] = \sum_m \Lambda_{nm}||\boldsymbol{d}^{nm}_{\text{exp.}}|^2 - |\boldsymbol{d}^{nm}_{\text{calc.}}|^2|^2$, being Λ_{nm} the amplitude of the dipole moment minimization. The equation obtained from varying $|\Psi_n\rangle$ in Eq. (13) around the stationary point is:

$$\hat{H}\,|\Psi_n\rangle + \sum_m \hat{V}^{nm}_{\text{d, exp.}}\,|\Psi_m\rangle = E_n\,|\Psi_n\rangle\,, \tag{14}$$

$$\hat{V}^{nm}_{\text{d, exp.}} = \Lambda_{nm}\left(|\boldsymbol{d}^{nm}_{\text{exp.}}|^2 - |\boldsymbol{d}^{nm}_{\text{calc.}}|^2\right)\boldsymbol{d}^{nm*}_{\text{calc.}}\cdot\hat{\boldsymbol{d}}. \tag{15}$$

Eq. (14) is the equation that we wish to solve in this project. To do so, we make use of a HF algorithm similar to the one described above, but including now our new potential term $\hat{V}^{nm}_{\text{d,exp.}}$. A more detailed derivation of the explicit expression of the new Fock matrix can be found in App. A.

Similarly, another coupled restrain we wish to introduce into our system is the forced orthogonalization that guarantees that no two states will collapse into one of them. In this case, the Eq. (14) would need a new potential $\hat{V}^{nm}_{\text{or,exp.}}$ that fits the operator $\hat{\mathbb{1}}$. This forces the set of excited states to be as orthogonal as possible, in the same way as the potential for the dipole moment would make the potential fit the experimental value as close as possible.

It is of high importance that we mention here how the sign of Λ_{nm} is crucial when seeking stationary states. In the case of the ground state, the stationary state is always an absolute minimum, and therefore a positive multiplier shall be used. Nonetheless for excited states there exists the possibility of encountering stationary points that are maxima as well, and in those cases negative Λ_{nm} will be needed. In the cases where the excited states correspond to saddle points of the Hamiltonian, we suggest using different signs of Λ_{nm} for each iteration, even though this case is beyond the scope of this project.

3. Computational Results

3.1. Structure of the code

Even though initially the programming language used was python, the code was finally programmed in Julia. We make use of Python-based Simulations of Chemistry Framework (PySCF) [13] library to obtain the matrix elements of our fundamental operators in the atomic orbital basis, such as the kinetic operator, the nuclear potential energy operator, etc; for a given molecule in a given specified atomic basis (some examples of atomic basis sets can be found in Basis Set Exchange). The calculation of the nucleus-nucleus energy is also included in the total energy of the system[3].

---

[3] This might allow to compute quantities such as the internuclear distance.

The first step given a specified molecule, is to obtain these operator elements using PySCF library, and use them to compute the ground state of the molecule. In order to obtain the excited ionized states from the ground state, as a first approximation we remove one electron (arbitrarily chosen as spin-down electron) from each occupied molecular orbital. This gives a total of N_β excited states that will serve as initial guesses to our restrained SCF algorithm[4], and the notation $|\Psi_n\rangle$ will be used to refer to the excited state that has removed the electron from the n^{th} orbital.

3.2. Experimentally restrained minimization

Let us focus our attention into our suggested example: a water molecule, formed by two Hydrogen and one Oxygen atom. The atomic basis set sto-6g [12] will be used throughout this section to simplify the calculation. In order to exemplify the results of our model, we will use the transition depicted in Fig. 1. The first step after obtaining the ground state, is to remove one electron from the first and fifth energetic levels $[(n,m) = (1,5)]$, such that a hole is left behind. These states now go through a relaxation process without any restrain, which allows us to estimate the unfitted relaxation of the states as well as the dipole moment of the pair, $\boldsymbol{d}^{15}_{\text{estim.}}$ [5]. We will use a shift of 5% and 9% in our specific example (these will be our test "experimental" dipole moments), and we will see how the error value evolves as we smoothly increase the value of Λ_{15} [6]. The formula used for the error of the dipole moment is[7]:

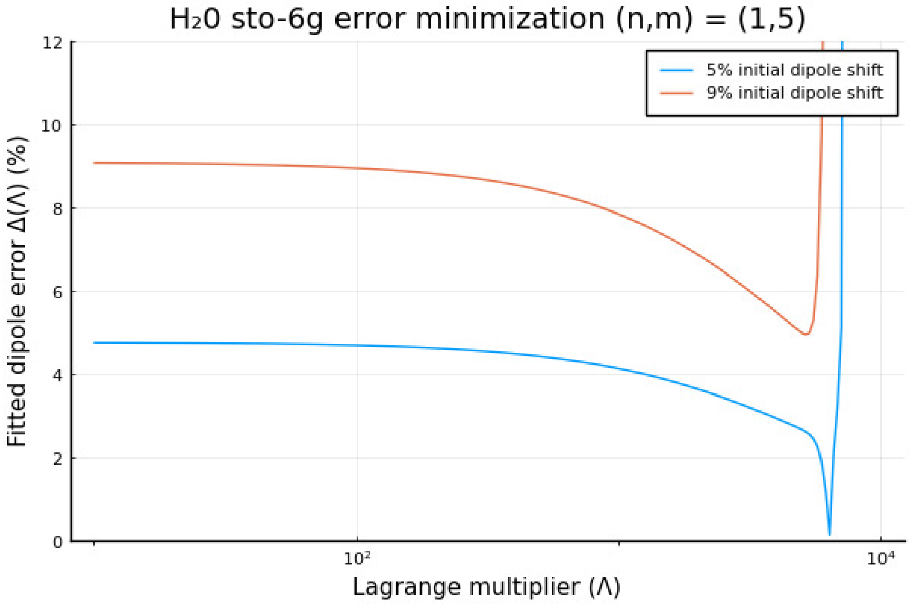

Figure 2: Graph representing the error of the fitted dipole moment Δ vs. the value of the Lagrange multiplier used Λ. A decrease in the error is observed when the Lagrange multiplier is increased, even though after a certain value of Λ the error increases rapidly and the algorithm loops.

$$\Delta(\Lambda) = \frac{|\boldsymbol{d}^{15}_{\text{exp.}} - \boldsymbol{d}^{15}_{\text{calc.}}(\Lambda)|}{|\boldsymbol{d}^{15}_{\text{exp.}}|} \times 100, \tag{16}$$

---

[4] Note that this initial guesses are essential for MOM to be implemented.

[5] Since we do not have yet the experimental values of the dipole moment, we will instead shift slightly the obtained dipole moment from the previous calculation

[6] As mentioned in earlier sections, the sign of off-diagonal Λ_{nm} is crucial to our description of the system. To make sure that the sign is correct, a first computation of non-fitting dipole moment excited states will be performed. Once convergence has been reached, we can use how the energy varies to determine the sign of Λ_{nm}: if energy decreases, the sign will be positive; if energy increases, the sign will be negative. This non-fitting states will also be used to get the order of magnitude of the dipole moment. In our case, $n = 1$ and $m = 5$, the sign of Λ_{15} turns out to be negative.

[7] Henceforth, the notation $\Lambda = |\Lambda_{15}|$

where $\boldsymbol{d}^{15}_{\text{calc.}}(\Lambda)$ represents the calculated dipole moment after the restrained minimization has been realized for a given value of Λ, and $\Delta(0) = \Delta_{\text{init.}}$, which in our case corresponds to 5% and 9%. in Fig. 2 we can observe the decrease of the error Δ with respect to the increase in the absolute value of the coupling Λ. The minimum value of the error is reached at 0.3% for the initial 5% shift, and 5% for the initial 9% shift. After a certain value of Λ, we can see in Fig. 2 a divergence. This is due to limitations of our model to perform the restrained minimization: the SCF algorithm used is not capable of finding the global minimum where $\Delta = 0\%$ and diverges.

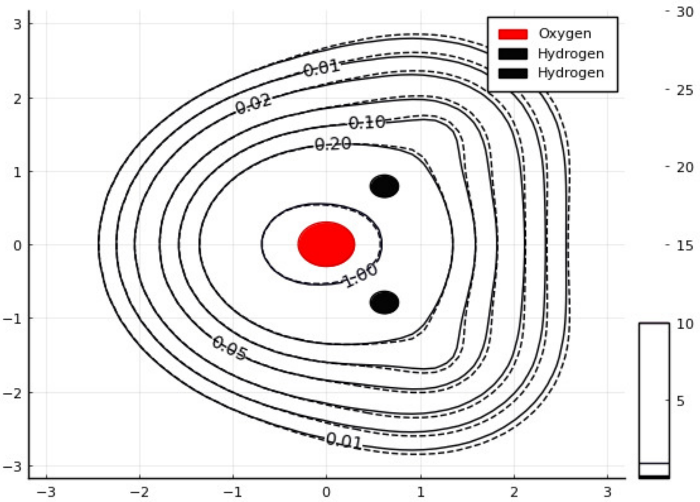

Figure 3: Graph representing the spatial density distribution of the total electronic density. The atoms are represented as circles: red and black for Oxygen and Hydrogen, respectively. The dashed line represents the unfitted density ($\Delta = 50\%$), while the solid line represents the fitted one ($\Delta = 5\%$). We have used $\Lambda = 5 \times 10^3$. The change is more pronounced far from the nuclei because outer orbitals contribute the most to the dipole moment.

We are also interested to see changes in the shape of the electronic density and orbitals. Since the changes a very subtle, we will use an extreme case of a 50% initial shift and $\Lambda = 5 \times 10^3$, and we will only represent the state $n = 1$. The resulting fitted states have an error of $\Delta = 5\%$. Fig. 3 is a representation of the 2D plane of the water molecule. The dashed line represents the unfitted density, while the solid line represents the fitted density. A subtle but consistent change in the shape can be seen in the electronic density. The change is more pronounced far from the nuclei because outer orbitals contribute the most to the dipole moment. Additionally, in Fig. 4 the comparison of the fitted and unfitted outer molecular orbitals can be found. Core orbitals do not contribute to the dipole moment, and thus their shape does not change whatsoever when this observable is fitted.

3.3. General discussion of the results

The implemented code contains many features that allow the results to remain as physical as possible. First, spin contamination in the excited is essential when the third component of the spin is very low (such is the case for $S_z = 0$ or $S_z = 1/2$), as there are more possible combinations of eigenstates of $\hat{S}^2$ that would produce such states. Another problem encountered was the collapse of different excited states into the same state, which was solved using the same formalism we used for the dipole moment fitting. These two problems: spin contamination and forced orthogonalization, have their respective restrain parameter λ, which is a free parameter and needs to be chosen according to the best behaviour of these two effects. Finding the correct set of $\boldsymbol{\lambda}$ for each specific case becomes a harder task when more than two states are coupled and the number of electrons is large.

X-ray absorption is, in principle, also a possible implementation of our code. Nevertheless (as discussed in App. B), the determination of the wavefunction in the continuum for the ejected electron

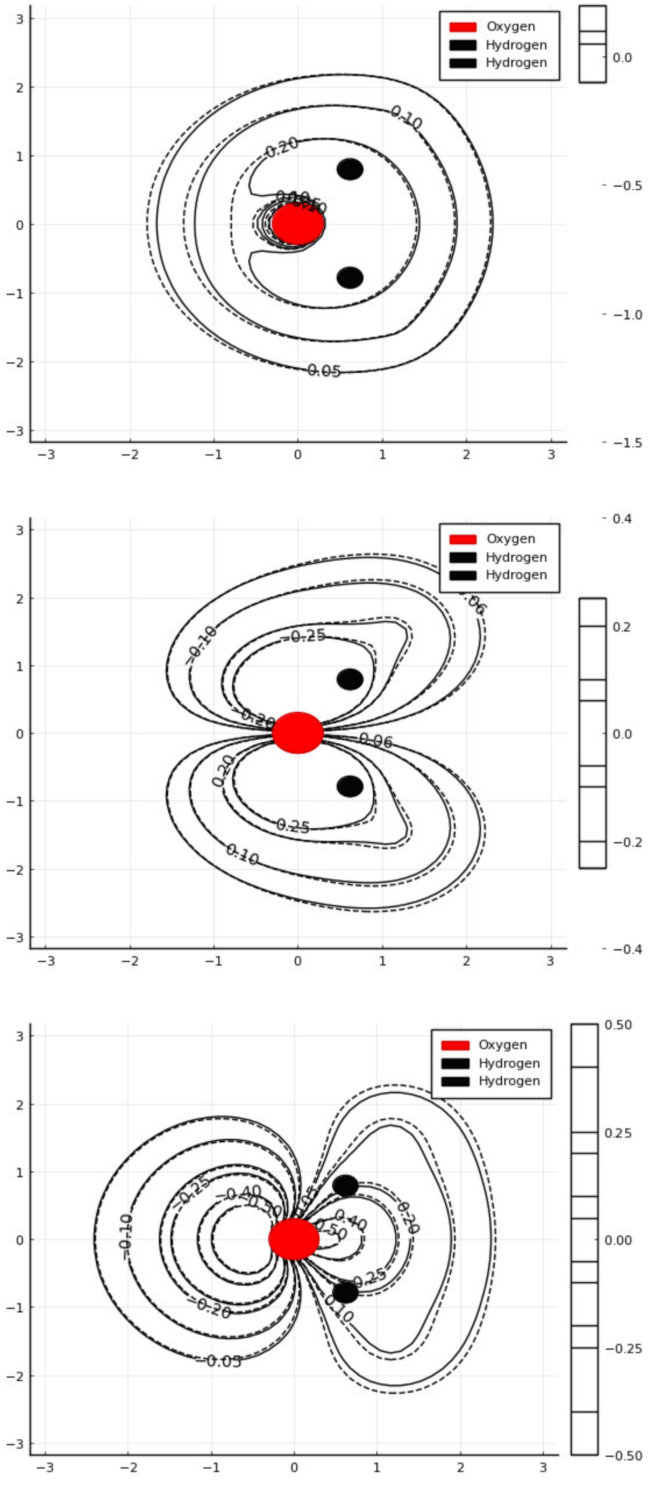

Figure 4: Graph representing the spatial distribution of the outer orbitals of the water molecule $n = 1$ state. The atoms are represented as circles: red and black for Oxygen and Hydrogen, respectively. The dashed line represents the unfitted orbital ($\Delta = 50\%$), while the solid line represents the fitted orbital ($\Delta = 5\%$). We have used $\Lambda = 5 \times 10^3$.

became an issue hard to solve, and that would require a special treatment, probably involving a numerical solution.

In general, the implemented code decreases the distance between the theoretical and the experimental dipole moment, keeping close attention to the sign used for the Lagrange multiplier $\Lambda_n m$ (positive for minimization, negative for maximization). The numerical results vary significantly with the chosen basis set, the molecule used, and the pair of excited states involved in the transition. Smaller basis sets tend to be more flexible to changes, and thus allow for a better fitting. This might be due to the fact that smaller basis sets are less precise when it comes to reaching a minimum and shifts from it are not hard to achieve, whereas in bigger basis sets the accuracy of the algorithm does not allow big changes. Although Fig. 2 represents a specific case, the same dependence on the Lagrange multiplier can be seen in many other situations, which leads us to think that choosing Λ_{nm} is, again, a minimization problem that might be hard to solve for more complex systems, since some values of Λ_{nm} might fit well for certain states but make others diverge. Our conclusion is that, even though the code was implemented for a very simple case, there is an open window to better techniques that can improve the accuracy and effectiveness of our model, and maybe tackle more complex systems that involve more fitting parameters.

4. Conclusion

Approximations in quantum many-body problems usually involve losing substantial information about the system, such as removing electron-electron correlations, or using finite atomic basis sets to perform calculations. Through this text, we have introduced a new algorithm within the Hartree-Fock formalism that allows to fit a set of experimentally measured parameters into our theoretical model. Specifically, we have focused ourselves on the idea of electric dipole moment fitting, which can be obtained from X-ray absorption and emission processes (as in Fig. 1). We have shown in this project that such algorithm is possible, as can be seen in the error decrease of in Fig. 2, which proves that experimental fitting is possible even in the simple case of Hartree-Fock-based algorithms. A significant change can also be observed in the electronic density (Fig. 3) and molecular orbitals (Fig. 4) when the difference between the observed experimental dipole moment and the unfitted one is notable. Even though we have restricted ourselves with electronics molecular transitions, the same basic idea can be used to coupled molecular states with different numbers of electrons in the molecule, as is the case of X-ray ionization (Fig. 1). Moreover, a general framework can be extracted from this project, that would allow for many improvements in the determination of the molecular wavefunctions using other experimental observables, and different formalisms from that of Hartree-Fock, such as those of DFT.

Acknowledgements

We acknowledge the technical support of Emanuelle Rossi (FS-TUXS) to obtain the spatial distribution of Fig. 3 and 4, as well as providing feedback input that helped the progress of the code. We also appreciate the financial support of Deutsches Elektronen-Synchrotron DESY Summer Student Programme for allowing the realization of this project.

References

[1] J. S. Andews, D. Jayatilaka, R. G. A. Bone, N. C. Handy, and R. D. Amos, *Spin contamination in single-determinant wavefunctions*, Chem. Phys. Let. **183**, 5 (1991) 423-431.

[2] A. T. B. Gilbert, N. A. Besley, and P. M. W. Gill, *Self-Consistent Field Calculations of Excited States Using the Maximum Overlap Method*, J. Phys. Chem. A **2008**, 112, 13164-13171.

[3] A. Szabo, N. S. Ostlund, *Modern Quantum Chemistry: Introduction to Advanced Electronic Structure Theory*, 1996.

[4] P. Pulay, *Improved SCF Convergence Acceleration*, J. Comp. Chem. **3**, 4, (1982) 556-560.

[5] P. Pulay, *Convergence Acceleration of Iterative Sequences. The Case of SCF Iteration*, Chem. Phys. Let. **73**, 2, (1980), 393-398.

[6] F. de Groot, A. Kotani, *Core Level Spectroscopy of Solids*, 2008.

[7] L. D. Landau, E. M. Lifshitz, *Course on Theoretical Physics Vol. III, Quantum Mechanics: Non-Relativistic Theory*, 1977.

[8] U.Bergmann, P. Glatzel, *X-Ray Emission Spectroscopy*, Photosynth. Res., **102**, 255 (2009).

[9] D.Jayatilaka, D. J. Grimwood, *Wavefunctions Derived from Experiment. I. Motivaion and Theory*, Acta Cryst. (2001) A**57**, 76-86.

[10] C. D. Sherrill, *Hartree-Fock Program Project.* Notes by Dr. Ykio Yamaguchi (University of Chicago).

[11] W. Koch, M. C. Holthausen, *A Chemist's Guide to Density Functional Theory*, 2001.

[12] B. P. Pritchard, D. Altarawy, B. Didier, T. D. Gibson, T. L. Windus, *A New Basis Set Exchange: An Open, Up-to-date Resource for the Molecular Sciences Community*, J. Chem. Inf. Model. 2019, **59** (11), 4814-4820.

[13] Q. Sun et al., *PySCF: the Python-based simulations of chemistry framework*, WIREs Comput. Mol. Sci. **8**, e1340 (2018).

A. Restrained Minimization Formulae

In this section, we will provide a sketch for the derivation of the formulae used in the code to make the computed dipole moment fit the experimentally measured dipole moment.

A.1. ECW

Our system is composed of a set of multi-electronic states $\{|\Psi_n\rangle\}$, and a set of operator $\hat{A}$ whose matrix elements, $A^{nm} = \langle\Psi_n|\hat{A}|\Psi_m\rangle$, are known. We define the quantity $Q[\{|\Psi_n\rangle\}]$ as the error between the experimental matrix element of the different operators $\hat{A}$ and its value for the set of states $\{|\Psi_n\rangle\}$:

$$Q_n[|\Psi_n\rangle] = \sum_{A,m} \Lambda^A_{nm} ||A^{nm}_{\text{exp.}}|^2 - |A^{nm}|^2|^2. \tag{17}$$

Our coupled system will be the result of an eigenvalue problem in which not only the classical Hartree-Fock Hamiltonian $\hat{H}$ will play a role, but we will also include a new interaction term between the different excited states that will make the system fit the matrix elements A^{nm}. Such Hamiltonian is derived from applying the variational theorem to the following Langrangian:

$$L_n[|\Psi_n\rangle] = \langle\Psi_n|\,\hat{H} - E_n\,|\Psi_n\rangle + Q^{\text{d}}_n[|\Psi_n\rangle], \tag{18}$$

which leads to

$$\hat{H}\,|\Psi_n\rangle + \sum_m \hat{V}^{nm}_{\text{exp.}}\,|\Psi_m\rangle = E_n\,|\Psi_n\rangle\,, \tag{19}$$

with the new potential being

$$\hat{V}^{nm}_{\text{exp.}} = \sum_A \frac{\partial Q}{\partial A^{nm}}\hat{A}. \tag{20}$$

A.2. Second quantization

To do the calculations, we will restric ourselves with the framework of second quantization, in which creation and anihilation operators for a given basis are used to define the operators. In our case, the operators look like:

$$\hat{H} = \sum_{p,q} h_{pq}\hat{a}^\dagger_p\hat{a}_q + \sum_{p,q,r,s} w_{pqrs}\hat{a}^\dagger_p\hat{a}^\dagger_q\hat{a}_s\hat{a}_r, \tag{21}$$

$$\hat{A} = \sum_{p,q} a_{pq}\hat{a}^\dagger_p\hat{a}_q, \tag{22}$$

where h_{pq} accounts for the one-electron part of the Hamiltonian, i.e., electron-nuclei interaction, kinetic operator, and nuclei-nuclei interaction; and w_{pqrs} represents the electron-electron interaction. The operator $\hat{A}$ is taken here as a one-electron operator. Using this formalism it will not be difficult to compute the matrix elements

A.3. Hartree-Fock

A.3.1. Definition of the states

Since we are working under the Hartree-Fock approximation, all multi-electornic states are single Slater determinants. The different molecular orbitals will be labeled with the state they correspond to, so that $|\psi_p^n\rangle$ refers to p molecular orbital of the state n.

$$|\Psi_n\rangle = \frac{1}{\sqrt{N_n!}} \det\left(|\chi_1^{(n)}\rangle\, |\chi_2^{(n)}\rangle\, |\chi_3^{(n)}\rangle \dots\right). \tag{23}$$

As explained in the main body, these states can be expressed in terms of atomic orbitals using the coefficient matrices $\{|\phi_p\rangle\}$:

$$|\psi_p^{\alpha(n)}\rangle = |\phi_\nu\rangle\, C_{\nu p}^{\alpha(n)} \tag{24}$$

$$\langle\phi_\mu|\phi_\nu\rangle = S_{\mu\nu} \tag{25}$$

A.3.2. Second quantization in different basis sets

The change of basis from one set to another can be expressed in terms of spin orbitals as:

$$\hat{a}_p^{(n)} = \langle\chi_p^{(n)}|\chi_q^{(m)}\rangle\, \hat{a}_q^{(m)} = C_{p\nu}^{(n)\dagger} S_{\nu\mu} C_{\mu q}^{(m)} \hat{a}_q^{(m)} \tag{26}$$

A.3.3. Observables

Using the fact that the states are made out of a single Slater determinant, we can find the formula for the matrix element of the observable $\hat{A}$. To do so, we define a new object we call *one-electron density matrix* $\gamma_{\mu\nu}^{nm}$:

$$A^{nm} = \langle\Psi_n|\, \hat{A}\, |\Psi_m\rangle = C_{a\nu}^{(n)\dagger} A_{\nu\mu} C_{\mu b}^{(m)} \langle\Psi_n|\, \hat{a}_a^{(n)\dagger} \hat{a}_b^{(m)}\, |\Psi_m\rangle = A_{\nu\mu}\left(\gamma_{\mu^\alpha\nu^\alpha}^{mn} + \gamma_{\mu^\beta\nu^\beta}^{mn}\right), \tag{27}$$

whose form in terms of coefficient and overlap matrices:

$$\gamma_{\mu\nu}^{\alpha,\beta mn} \equiv \gamma_{\mu^{\alpha,\beta}\nu^{\alpha,\beta}}^{mn} = C_{\mu a}^{\alpha,\beta(m)} \mathrm{Cofactor}_{b,a}\left(\left\{C_{c\sigma}^{\alpha,\beta(n)\dagger} S_{\sigma\delta} C_{\delta d}^{\alpha,\beta(m)}\right\}\right) \det\left(\left\{C_{c\sigma}^{\beta,\alpha(n)\dagger} S_{\sigma\delta} C_{\delta d}^{\beta,\alpha(m)}\right\}\right) C_{b\nu}^{\alpha,\beta(n)\dagger}. \tag{28}$$

It can be proven that the case when $n = m$ corresponds to the density matrix of state n:

$$\gamma_{\mu^{\alpha,\beta}\nu^{\alpha,\beta}}^{nn} = D_{\mu\nu}^{\alpha,\beta(n)} = C_{\mu a}^{\alpha,\beta(n)} C_{a\nu}^{\alpha,\beta(n)\dagger}, \tag{29}$$

We will also need to define a *two-electron density matrix* to compute the Hamiltonian (written with spin orbital indices):

$$\gamma_{\mu\nu\mu'\nu'}^{mn} = C_{\mu a}^{(m)} C_{\nu b}^{(m)} \mathrm{Cofactor}_{a'b',ab}\left(\left\{C_{c\sigma}^{(n)\dagger} S_{\sigma\delta} C_{\delta d}^{(m)}\right\}\right) C_{a'\mu'}^{(n)\dagger} C_{b'\nu'}^{(n)\dagger}. \tag{30}$$

To obtain the spatial orbital expression, one needs to explicitly substitute all possible combinations of α adn β. Only the following combinations have an actual contribution in our problem: $\gamma_{\mu\nu\mu'\nu'}^{\alpha\alpha mn} \equiv \gamma_{\mu^\alpha\nu^\alpha\mu'^\alpha\nu'^\alpha}^{mn}$, $\gamma_{\mu\nu\mu'\nu'}^{\alpha\beta mn} \equiv \gamma_{\mu^\alpha\nu^\beta\mu'^\alpha\nu'^\beta}^{mn}$, $\gamma_{\mu\nu\mu'\nu'}^{\beta\alpha mn} \equiv \gamma_{\mu^\beta\nu^\alpha\mu'^\beta\nu'^\alpha}^{mn}$, and $\gamma_{\mu\nu\mu'\nu'}^{\beta\beta mn} \equiv \gamma_{\mu^\beta\nu^\beta\mu'^\beta\nu'^\beta}^{mn}$. The total energy of the system remains the same as in the traditional Hartree-Fock case [3] (using the definition of traditional Fock operator given in Eq. (4))

$$E^{(n)} = \frac{1}{2}\left[h_{\mu\nu}\left(D_{\nu\mu}^{\alpha(n)} + D_{\nu\mu}^{\beta(n)}\right) + F_{\mu\nu}^{\alpha} D_{\nu\mu}^{\alpha} F_{\mu\nu}^{\beta} D_{\nu\mu}^{\beta}\right]. \tag{31}$$

A.4. Brillouin's theorem

A very important theorem of quantum theory within Hartree-Fock approximation will be used here to obtain the matrix elements of our potential term $\hat{V}_{\text{exp.}}$. The theorem goes likes this: *singly excited determinants* $\hat{a}_i^{(n)\dagger}\hat{a}_a^{(n)}\left|\Psi_n\right\rangle$ *will not interact directly with a arefrence Hartee-Fock determinant* $\left|\Psi_n\right\rangle$[8]:

$$\left\langle\Psi_n\right|\hat{a}_a^{(n)\dagger}\hat{a}_i^{(n)}\hat{H}\left|\Psi_n\right\rangle+\sum_{A,m}\frac{\partial Q}{\partial A^{nm}}\left\langle\Psi_n\right|\hat{a}_a^{(n)\dagger}\hat{a}_i^{(n)}\hat{A}\left|\Psi_m\right\rangle+\sum_{S,m}\frac{\partial Q}{\partial S^{nm}}\left\langle\Psi_n\right|\hat{a}_a^{(n)\dagger}\hat{a}_i^{(n)}\left|\Psi_m\right\rangle=0. \tag{32}$$

Note that the potential has been writen explicitly from Eq. (20) for the operators $\hat{A}$ and $\hat{\mathbb{1}}$, the former will refer to the dipole moment while the latter refers to the overlap (to avoid collapse between excited states).

A.4.1. Traditional Fock matrix

We can use the traditional Fock operator derived in [3], which is related to the Hamiltonian $\hat{H}$ (written in spin orbital form):

$$F_{pq}^{(n)}=h_{pq}^{(n)}+\left(w_{pbqb}^{(n)}-w_{pbbq}^{(n)}\right)=C_{p\mu}^{(n)\dagger}\left[h_{\mu\nu}+\left(w_{\mu\mu'\nu\nu'}-w_{\mu\mu'\nu'\nu}\right)D_{\nu'\mu'}^{(n)}\right]C_{\nu q}^{(n)}$$

A.4.2. v-o block

Only virtual-occupied matrix elements, or viceversa, will have an actual contribution to the extended Fock matrix of the system (written in spin orbital form):

$$\bar{F}_{ia}^{(n)}=F_{ia}^{(n)}+\sum_{m\neq n}v_{ia}^{(n,m)}=0, \tag{33}$$

$$v_{ia}^{(n,m)}=\frac{\partial Q}{\partial A^{nm}}C_{i\sigma}^{(n)\dagger}\left[A_{\sigma\nu}\gamma_{\nu\mu}^{mn}+S_{\sigma\nu}\gamma_{\nu\mu'\mu\nu'}^{mn}A_{\nu'\mu'}\right]S_{\mu\delta}C_{\delta a}^{(n)}+\frac{\partial Q}{\partial S^{nm}}C_{i\sigma}^{(n)\dagger}S_{\sigma\nu}\gamma_{\nu\mu}^{mn}S_{\mu\delta}C_{\delta a}^{(n)}. \tag{34}$$

To find the occupied-virtual matrix elements, it is only necessary to get the hermitian conjugate of these expressions. In the case of virtual-virtual and occupied-occupied case, the Fock matrix keeps the same form as it does in the traditional Hartree-Fock case.

$$\bar{F}_{ab}^{(n)}=F_{ab}^{(n)},\quad \bar{F}_{ij}^{(n)}=F_{ij}^{(n)}. \tag{35}$$

A.5. Atomic spin-orbitals

Finally, the last step is to compute the matrix elements in our atomic basis $\{\left|\phi_\mu\right\rangle\}$, which will be needed for the actual numerical computation:

$$\bar{F}_{\mu\nu}^{(n)}=F_{\mu\nu}^{(n)}+\sum_{m\neq n}v_{\mu\nu}^{(n,m)} \tag{36}$$

$$F_{\mu\nu}^{(n)}=h_{\mu\nu}+\left(w_{\mu\mu'\nu\nu'}-w_{\mu\mu'\nu'\nu}\right)D_{\nu'\mu'}^{(n)} \tag{37}$$

Accounting for the fact that only off-diagonal virtual-orbital terms contribute to the extended Fock matrix of the system, we arrive at the following formula for the potential in the atomic basis:

---

[8] Here, the subindex a represents occupied orbitals, and subindex i represents virtual orbitals. This way, only off-diagonal occupied-virtual orbitals will have a non-zero matrix element for the potential $\hat{V}_{\text{exp.}}$.

$$v_{\mu\nu}^{\alpha(n,m)} = \frac{\partial Q}{\partial A^{nm}} \left[\delta_{\mu\sigma} - S_{\mu\sigma'} D_{\sigma'\sigma}^{\alpha(n)}\right] \left[A_{\sigma\rho}\gamma_{\rho\kappa}^{\alpha mn} + S_{\sigma\rho}\gamma_{\rho\mu'\kappa\nu'}^{\alpha\alpha mn} A_{\nu'\mu'} + S_{\sigma\rho}\gamma_{\rho\mu'\kappa\nu'}^{\alpha\beta mn} A_{\nu'\mu'}\right] S_{\kappa\delta} D_{\delta\delta'}^{\alpha(n)} S_{\delta'\nu}$$
$$+ \frac{\partial Q}{\partial S^{nm}} \left[\delta_{\mu\sigma} - S_{\mu\sigma'} D_{\sigma'\sigma}^{\alpha(n)}\right] S_{\sigma\rho}\gamma_{\rho\kappa}^{\alpha mn} S_{\kappa\delta} D_{\delta\delta'}^{\alpha(n)} S_{\delta'\nu} + h.c. \tag{38}$$

$$v_{\mu\nu}^{\beta(n,m)} = \frac{\partial Q}{\partial A^{nm}} \left[\delta_{\mu\sigma} - S_{\mu\sigma'} D_{\sigma'\sigma}^{\beta(n)}\right] \left[A_{\sigma\rho}\gamma_{\rho\kappa}^{\beta mn} + S_{\sigma\rho}\gamma_{\rho\mu'\kappa\nu'}^{\beta\alpha mn} A_{\nu'\mu'} + S_{\sigma\rho}\gamma_{\rho\mu'\kappa\nu'}^{\beta\beta mn} A_{\nu'\mu'}\right] S_{\kappa\delta} D_{\delta\delta'}^{\beta(n)} S_{\delta'\nu}$$
$$+ \frac{\partial Q}{\partial S^{nm}} \left[\delta_{\mu\sigma} - S_{\mu\sigma'} D_{\sigma'\sigma}^{\beta(n)}\right] S_{\sigma\rho}\gamma_{\rho\kappa}^{\beta mn} S_{\kappa\delta} D_{\delta\delta'}^{\beta(n)} S_{\delta'\nu} + h.c. \tag{39}$$

B. X-ray absorption

The ground state of a molecule provides a lot of information about its structure. Such information is convenient in the field of quantum chemistry, as it would permit calculations that go beyond electronic models and could include nuclear positions as free parameters of our model, which in the case of excited states becomes a non-trivial task to perform. This is due to the absolute minimum nature of the ground state in the minimization problem. In the scope of our project, ground states can be studied by studying X-ray absorption processes (XAS), where one of the electron in the core is ejected by the absorption of an X-ray photon. This electron (which we will consider carries spin down), jumps to a state in the continuum spectrum, and this means that a precise solution to this wavefunction has to be found that permits a precise evaluation within the spatial scale of the molecule. Yet, we found difficulties when modelling the free electron wavefunction: the precision we need for the ejecte electron does not allow us to simply pick a plane or Coulomb wave, and therefore continuous energy levels need a special treatment that we could not develop in the scope of this project. We have, nevertheless, develop all the theoretical model needed to perform such a code in case these continuum wavefunctions would be included in the model.

Using the scketch portrayed in Fig. 1 for the ground state and the initial ionization, we can describe the two configurations involved in this model: initial state of N electrons: $|\Psi_i\rangle = |\Psi_n^{(N)}\rangle$, and final state of $N-1$ electrons: $|\Psi_f\rangle = |\Psi_m^{(N-1)}\rangle \otimes |\boldsymbol{k_e}, \beta\rangle$. The cross section of the X-ray absorption would then be [6]:

$$\sigma = \frac{c\mu_0\pi e^2}{\hbar m^2\omega} \sum_i w_i \int_f d\omega_f \delta(\omega_{fi} - \omega) |\boldsymbol{\epsilon} \cdot \boldsymbol{p_{fi}}(\boldsymbol{K})|^2 \tag{40}$$

$$\boldsymbol{p_{fi}} = \langle\Psi_f|\hat{\boldsymbol{p}}(\boldsymbol{K})|\Psi_i\rangle = \boldsymbol{p}_{\boldsymbol{k_e}q}^{(0)}(\boldsymbol{K}) \tag{41}$$

$$\hat{\boldsymbol{p}}(\boldsymbol{K}) = \int d^3\boldsymbol{k}_e \sum_q \left(\boldsymbol{p}_{\boldsymbol{k_e}q}^{(0)}(\boldsymbol{K}) \hat{a}_{\boldsymbol{k_e}}^\dagger \hat{a}_q + \boldsymbol{p}_{q\boldsymbol{k_e}}^{(0)}(\boldsymbol{K}) \hat{a}_q^\dagger \hat{a}_{\boldsymbol{k_e}}\right) \tag{42}$$

$$\boldsymbol{p}_{q\boldsymbol{k_e}}^{(0)}(-\boldsymbol{K}) \equiv \frac{1}{2} \langle\phi_q|\hat{\boldsymbol{p}} e^{-i\boldsymbol{K}\cdot\boldsymbol{r}} + e^{-i\boldsymbol{K}\cdot\boldsymbol{r}}\hat{\boldsymbol{p}}|\boldsymbol{k_e}\rangle \tag{43}$$

From this cross section, it would be possible to extract $\boldsymbol{p}_{q\boldsymbol{k_e}}^{(0)}(-\boldsymbol{K})$, and from it the dipole moment. The difficulty encountered in this model is how to determine $|\boldsymbol{k_e}\rangle$, i.e., the scattered electron wavefunction. Some suggestions would be using plane or Coulomb waves. However, these would differ from the actual result at distances close to the molecule, which are precisely those we are interested in. It is for this reason that we did not implement the code for this theory in much detail. If were to perform the calculation of the matrix elements of the potential $\hat{V}_{\text{exp.}}$ as we did in App. A, but with the peculiarity that now we are dealing with a final state involving an electron in continuum $|\Psi_f\rangle = |\Psi_m^{(N-1)}\rangle \otimes |\boldsymbol{k_e}, \beta\rangle$, we arrive at the following expressions:

$$
\begin{aligned}
v_{i^\alpha a^\alpha}^{(n,m)} &= -\frac{\delta Q}{\delta A^{nm}} C_{i\sigma}^{(n)\dagger\alpha} S_{\sigma\nu} \gamma^{mn}_{k_e^\beta \nu^\alpha \nu'^\beta \mu^\alpha} A^\beta_{\nu' k_e} S_{\mu\delta} C_{\delta a}^{(n)\alpha} \\
v_{i^\beta a^\beta}^{(n,m)} &= \frac{\delta Q}{\delta A^{nm}} C_{i\sigma}^{(n)\dagger\beta} \left\{ A^\beta_{\sigma k_e} \gamma^{mn}_{k_e^\beta \mu^\beta} - S_{\sigma\nu} \gamma^{mn}_{k_e^\beta \nu^\beta \nu'^\beta \mu^\beta} A^\beta_{\nu' k_e} \right\} S_{\mu\delta} C_{\delta a}^{(n)\alpha} \\
v_{i^\alpha a^\beta}^{(n,m)} &= v_{i^\beta a^\alpha}^{(n,m)} = 0
\end{aligned}
\tag{44}
$$